Supporting Information

Oxygen-dependent asparagine hydroxylation of the ubiquitin-associated (UBA) domain in Cezanne regulates ubiquitin binding

Julia Mader[1], Jessica Huber[2], Florian Bonn[1], Volker Dötsch[2], Vladimir V. Rogov[2], Anja Bremm[1]*

[1] Institute of Biochemistry II, Goethe University Frankfurt - Medical Faculty, University Hospital, Theodor-Stern-Kai 7, 60590 Frankfurt am Main, Germany
[2] Institute of Biophysical Chemistry and Center for Biomolecular Magnetic Resonance, Goethe University Frankfurt, Max-von-Laue Str. 9, 60438 Frankfurt am Main, Germany

*To whom correspondence should be addressed: bremm@em.uni-frankfurt.de

Content: Figures S1-S7

Figure S1

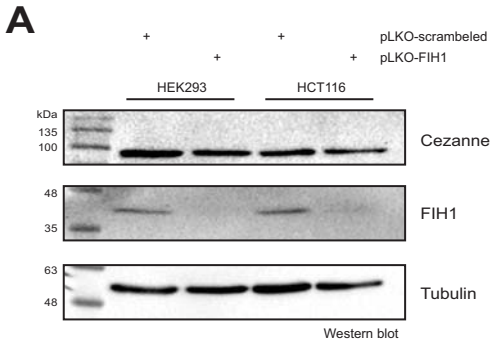
A
+
+
pLKO-scrambeled
+
+
pLKO-FIH1
HEK293
HCT116
kDa
135
100
Cezanne
48
35
FIH1
63
48
Tubulin
Western blot

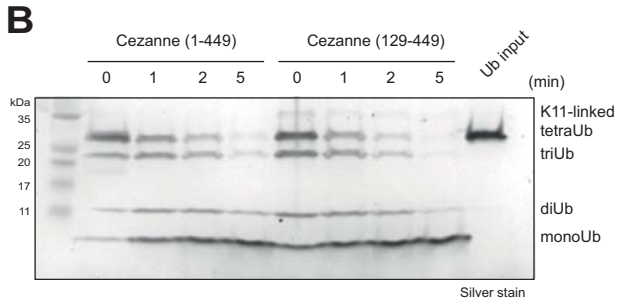
B
Cezanne (1-449)
Cezanne (129-449)
Ub input
0 1 2 5 0 1 2 5
(min)
kDa
35
25
20
17
11
K11-linked
tetraUb
triUb
diUb
monoUb
Silver stain

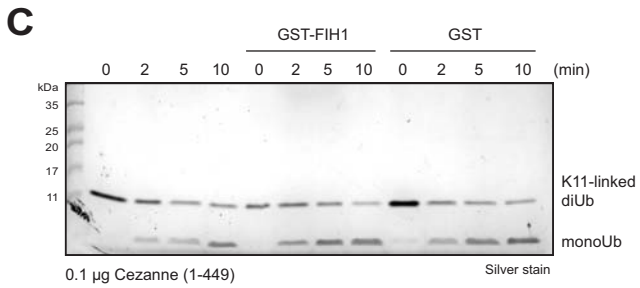
C
GST-FIH1
GST
0 2 5 10 0 2 5 10 0 2 5 10
(min)
kDa
35
25
20
17
11
K11-linked
diUb
monoUb
0.1 µg Cezanne (1-449)
Silver stain

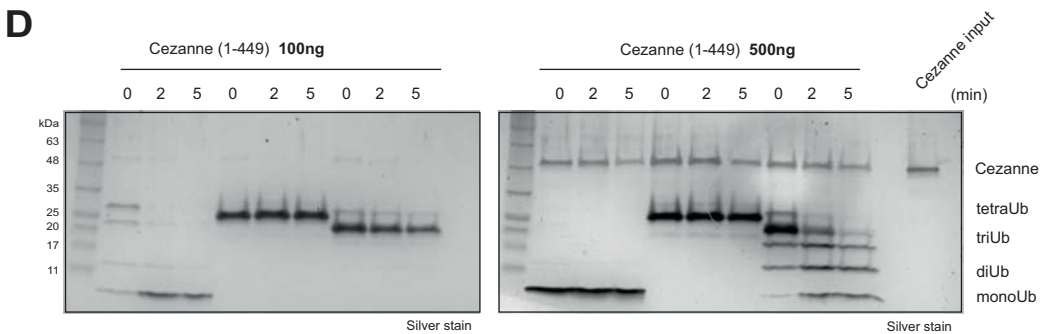
D
Cezanne (1-449) 100ng
Cezanne (1-449) 500ng
Cezanne input
0 2 5 0 2 5 0 2 5
0 2 5 0 2 5 0 2 5
(min)
kDa
63
48
35
25
20
17
11
Cezanne
tetraUb
triUb
diUb
monoUb
Silver stain
Silver stain

Figure S1: ***A***, Knockdown of FIH1 in HEK293 and HCT116 cells did not change Cezanne protein level. ***B***, *In vitro* cleavage assay of Lys11-linked diubiquitin by recombinant Cezanne comprising either the catalytic OTU domain alone (amino acids 129-449) or both the UBA and OTU domain (amino acids 1-449). ***C***, *In vitro* cleavage assay of K11-linked diubiquitin by recombinant Cezanne comprising the UBA and catalytic OTU domain (amino acids 1-449) in the presence and absence of recombinant FIH1. ***D***, *In vitro* cleavage assay of K11-, K48- and K63-linked tetraubiquitin by different amounts of recombinant Cezanne.

Figure S2

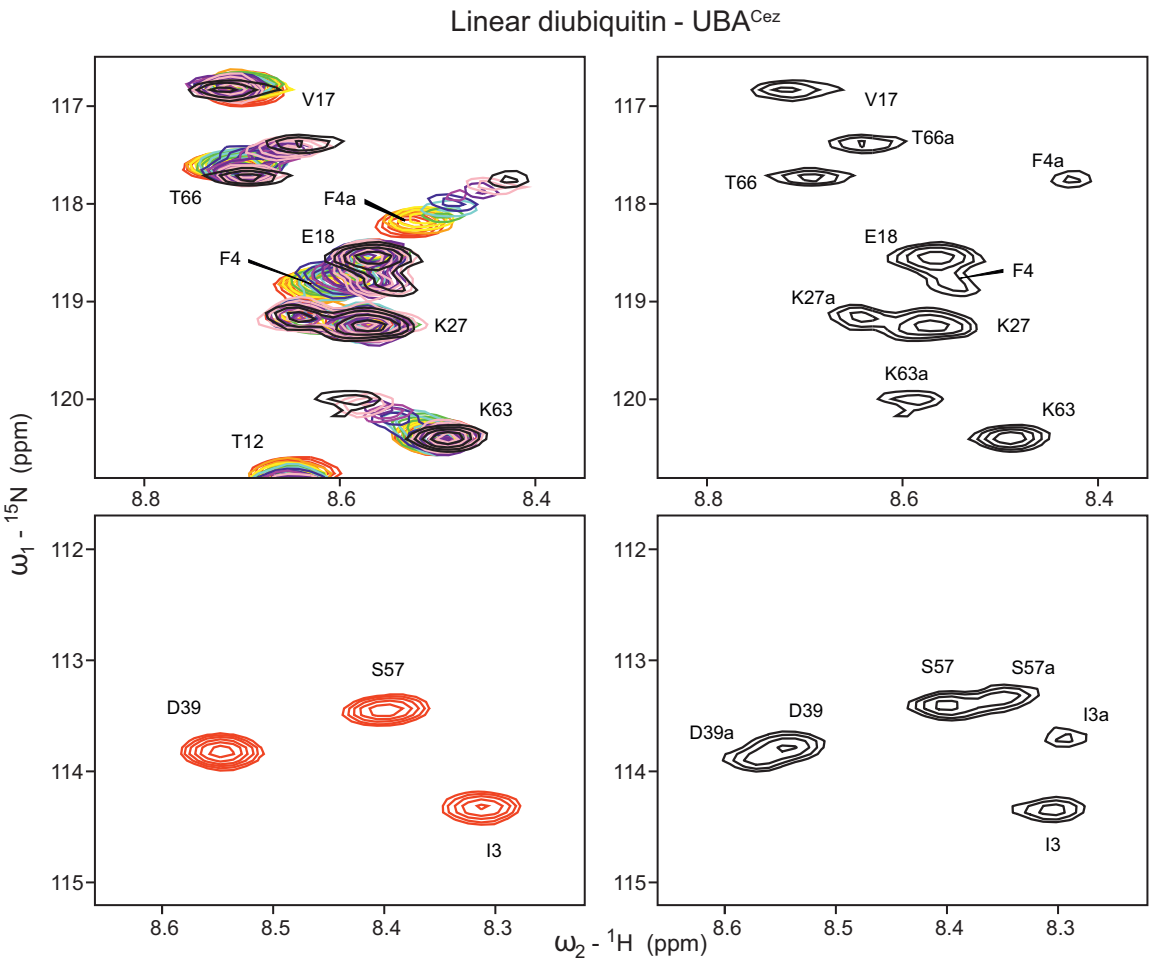
Linear diubiquitin - UBA^Cez
V17
T66
F4a
E18
F4
K27
K63
T12
V17
T66a
T66
F4a
E18
F4
K27a
K27
K63a
K63
D39
S57
I3
D39
S57
S57a
D39a
I3a
I3
ω1 - 15N (ppm)
ω2 - 1H (ppm)

Figure S2: Representative areas of [^{15}N,^{1}H]-BEST-TROSY HSQC spectra for ^{15}N-labelled linear diubiquitin upon titration with non-labelled UBA^{Cez}. Upper left: area near K63 and T66 HN resonances; the rainbow color code indicates increased molar ratios (defined in Figure 4a legend) upon titration from free linear diubiquitin (red) to full saturation upon 8-fold excess of UBA^{Cez} (dark grey). Upper right: The only area for the ^{15}N-labelled linear diubiquitin with 8-fold excess of UBA^{Cez} is shown. Note, that K63 and T66 backbone HN resonances evolved from single peaks in the free protein spectra to the two for each in UBA^{Cez} saturated spectra, with different intensities and CSP values for the observed sub-peaks. Representative area of [^{15}N,^{1}H]-BEST-TROSY HSQC spectra showing I3, D39 and S57 backbone HN resonances in free linear diubiquitin (lower left plot, red contours) and with 8-fold excess of UBA^{Cez} (lower right plot, dark grey contours).

Figure S3

All CSP on the distal Ub

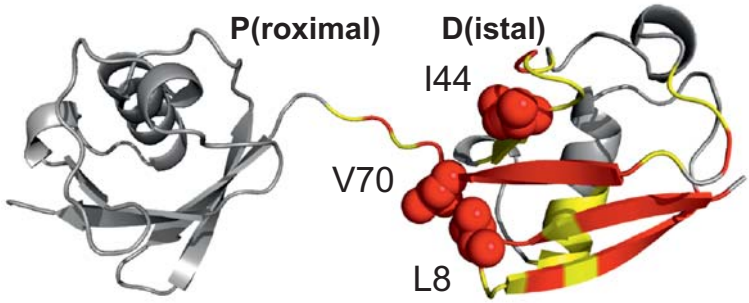

Filter out all „doublets“ in the spectra

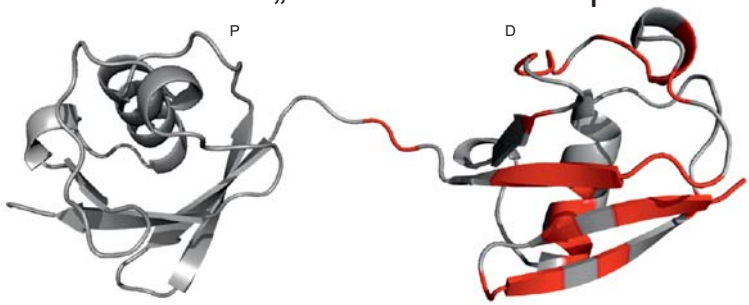

Resulting map on distal and proximal Ub

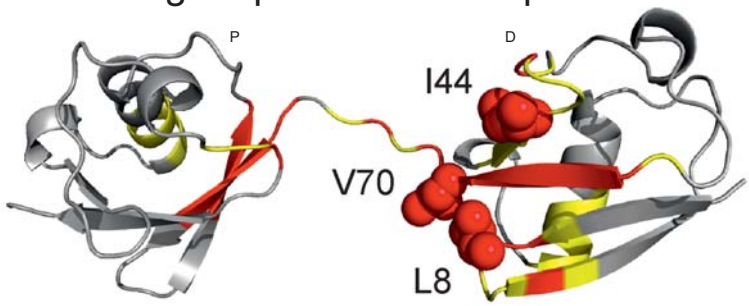

Figure S3: Assignment strategy for CSP mapping on distal and proximal ubiquitin moieties of linear diubiquitin. Calculated CSP upon titration with UBA^{Cez} were first mapped on the distal ubiquitin. Subsequently, all double peaks (shown red) were filtered out and resulting CSP were rationally (distance-based) mapped on the distal and proximal ubiquitin moiety, respectively. The yellow and red colors are defined in Figure 4g legend.

Figure S4

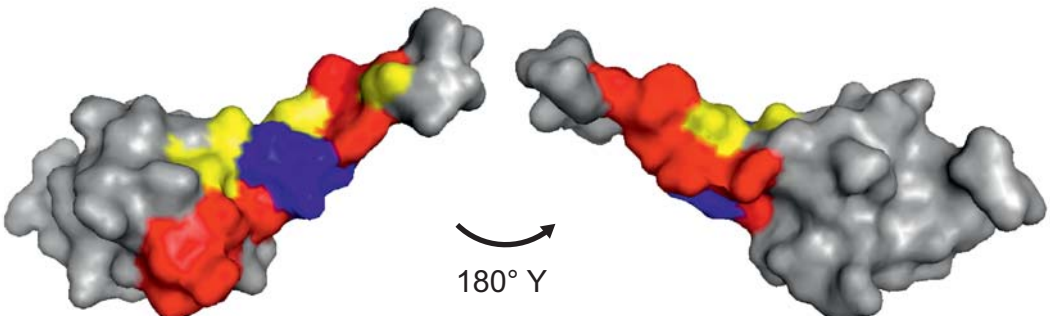

Figure S4: CSP mapping on the surface of the modelled UBA^{Cez} structure. Color code is described in Fig. 5*G*.

Figure S5

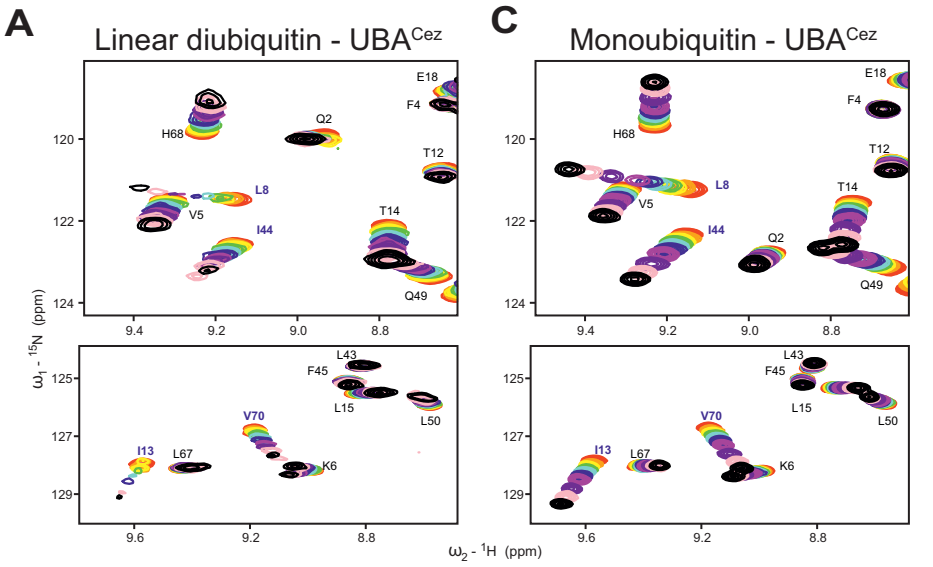
A
Linear diubiquitin - UBA^Cez
C
Monoubiquitin - UBA^Cez
ω1 - 15N (ppm)
ω2 - 1H (ppm)

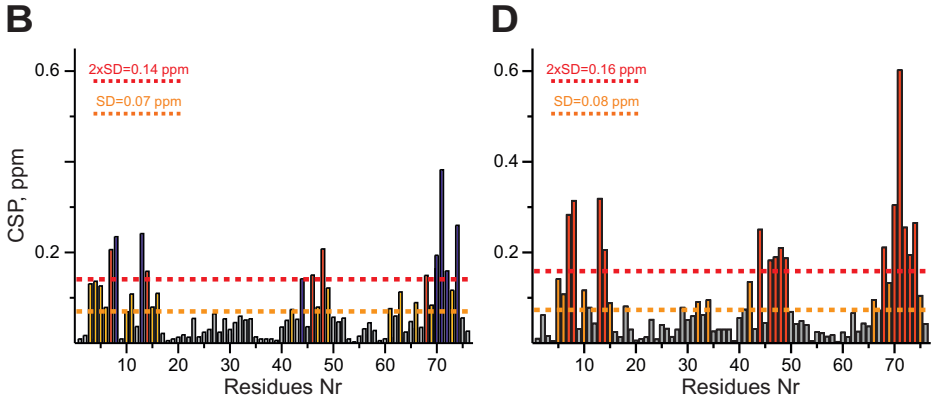
B
D
2xSD=0.14 ppm
SD=0.07 ppm
2xSD=0.16 ppm
SD=0.08 ppm
CSP, ppm
Residues Nr

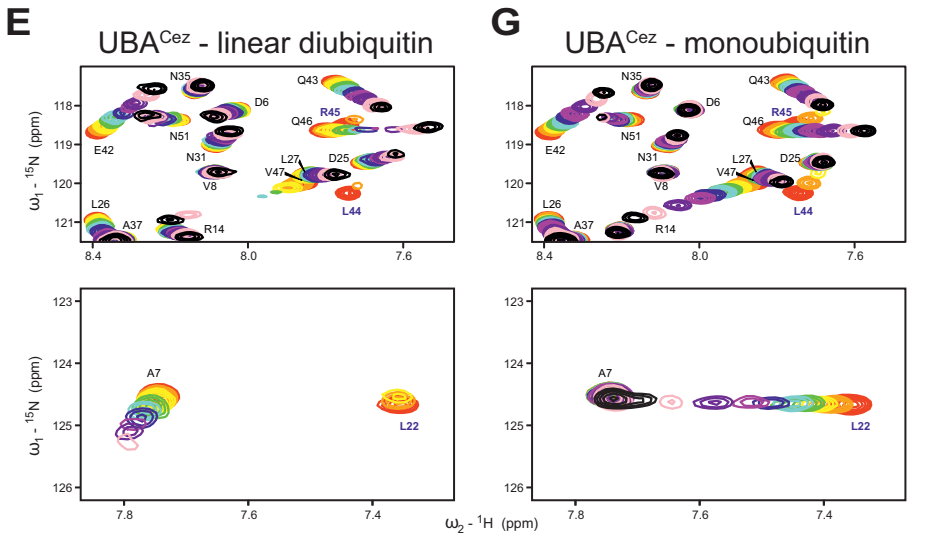
E
UBA^Cez - linear diubiquitin
G
UBA^Cez - monoubiquitin
ω1 - 15N (ppm)
ω2 - 1H (ppm)

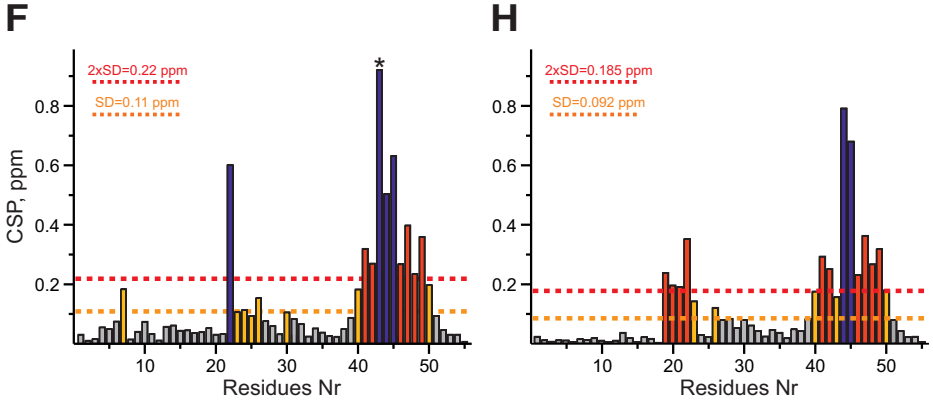
F
H
2xSD=0.22 ppm
SD=0.11 ppm
2xSD=0.185 ppm
SD=0.092 ppm
CSP, ppm
Residues Nr

Figure S5: Differences in the binding of linear diubiquitin and monoubiquitin to UBA^{Cez}. ***A***, NMR titration of ^{15}N-labelled linear diubiquitin with non-labelled UBA^{Cez}. Two representative areas of [^{15}N,^{1}H]-BEST-TROSY HSQC spectra are shown. ***B***, CSP mapping on the ubiquitin sequence. Yellow and red lines indicate the 1× and 2× standard deviations (δ) calculated from CSP values of all residues, respectively. Residues of linear diubiquitin, which showed double peaks (either in the free or in UBA^{Cez}-bound form) and significant line broadening, are colored in blue. ***C***, NMR titration of ^{15}N-labelled monoubiquitin with non-labelled UBA^{Cez}. The same areas are shown. ***D***, CSP mapping on the ubiquitin sequence. Yellow and red lines indicate the 1× and 2× standard deviations (δ) calculated from CSP values of all residues, respectively. There were no CSPs for monoubiquitin, which can be categorised as "blue". ***E***, NMR titration of ^{15}N-labelled UBA^{Cez} with linear diubiquitin. Two representative areas of [^{15}N,^{1}H]-BEST-TROSY HSQC spectra are shown. ***F***, CSP mapping on the UBA^{Cez} sequence. Yellow and red lines indicate the 1× and 2× standard deviations (δ) calculated from CSP values of all residues, respectively. Residues of UBA^{Cez}, which showed intermediate exchange and significant line broadening, are colored in blue. Asterisk indicates CSP for the side chain of Gln43, that shows intermediate and big CSP upon binding of linear diubiquitin. ***G***, NMR titration of ^{15}N-labelled UBA^{Cez} with monoubiquitin. The same areas are shown. Note that Ala7 backbone HN resonance being significantly perturbed in case of linear diubiquitin titration, is almost intact in case of monoubiquitin titration. For Leu22, titration with the diubiquitin induces more strong CSP (the resonance did not appear at the saturation point) with different direction (see the arrow at the corresponding plots). ***H***, CSP mapping on the UBA^{Cez} sequence. Yellow and red lines indicate the 1× and 2× standard deviations (δ) calculated from CSP values of all residues, respectively. Residues of UBA^{Cez}, which showed intermediate exchange and significant line broadening, are colored in blue.

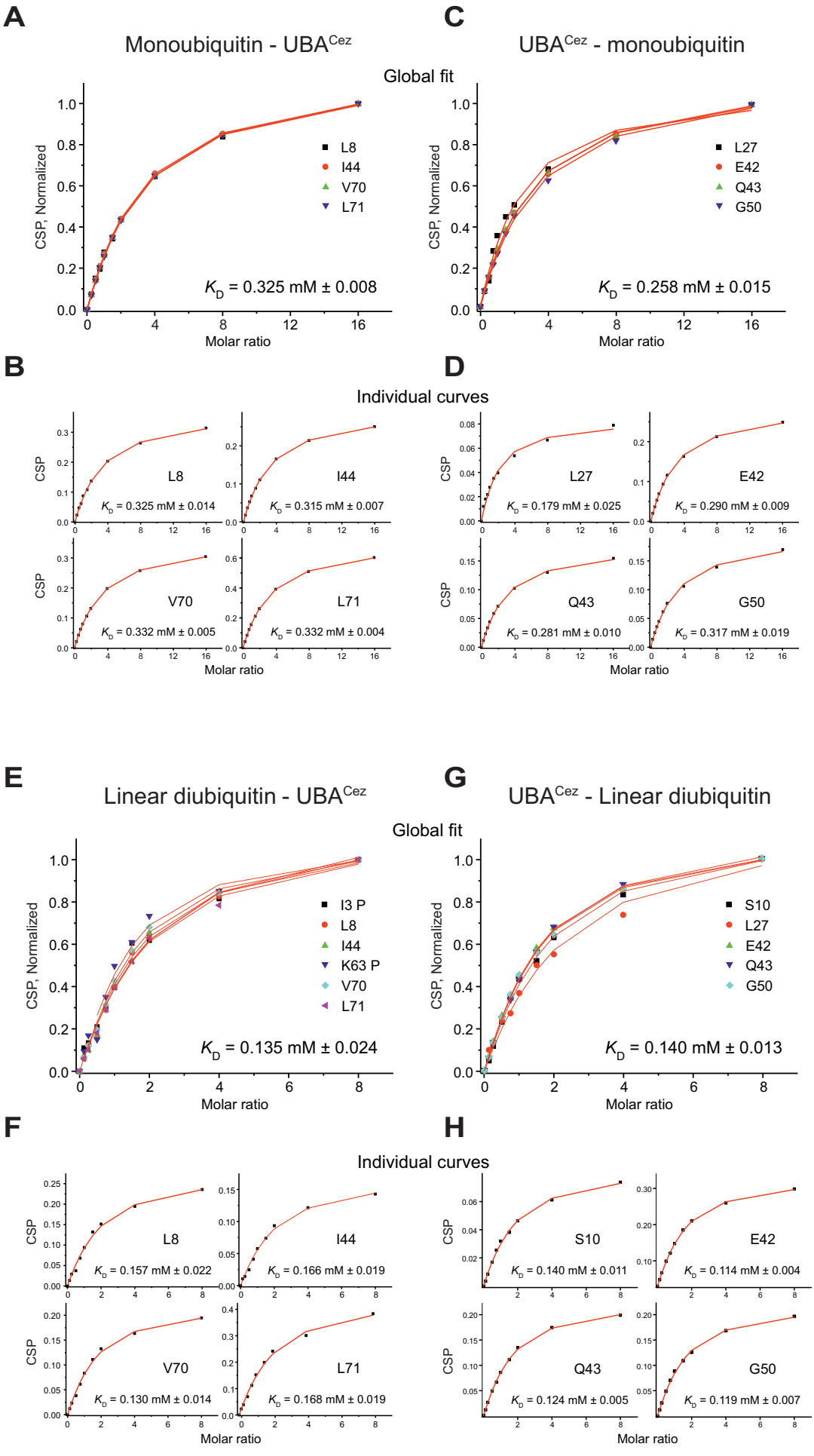
A
Monoubiquitin - UBA^Cez
Global fit
CSP, Normalized
Molar ratio
L8
I44
V70
L71
K_D = 0.325 mM ± 0.008
C
UBA^Cez - monoubiquitin
L27
E42
Q43
G50
K_D = 0.258 mM ± 0.015
B
Individual curves
CSP
L8
K_D = 0.325 mM ± 0.014
I44
K_D = 0.315 mM ± 0.007
V70
K_D = 0.332 mM ± 0.005
L71
K_D = 0.332 mM ± 0.004
D
L27
K_D = 0.179 mM ± 0.025
E42
K_D = 0.290 mM ± 0.009
Q43
K_D = 0.281 mM ± 0.010
G50
K_D = 0.317 mM ± 0.019
E
Linear diubiquitin - UBA^Cez
I3 P
K63 P
K_D = 0.135 mM ± 0.024
G
UBA^Cez - Linear diubiquitin
S10
K_D = 0.140 mM ± 0.013
F
L8
K_D = 0.157 mM ± 0.022
I44
K_D = 0.166 mM ± 0.019
V70
K_D = 0.130 mM ± 0.014
L71
K_D = 0.168 mM ± 0.019
H
S10
K_D = 0.140 mM ± 0.011
E42
K_D = 0.114 mM ± 0.004
Q43
K_D = 0.124 mM ± 0.005
G50
K_D = 0.119 mM ± 0.007

Figure S6: K_D calculations for the interaction between UBA^{Cez} and monoubiquitin (***A-D***) or linear diubiquitin (***E-H***). ***A***, Normalized CSP values of monoubiquitin residues Leu8, Ile44, Val70 and Leu71, showing significant CSP in the fast exchange mode, were used in the global fit. ***B***, Individual titration curves for the same residues. K_D values are indicated in each plot. ***C***, Normalized CSP values of UBA^{Cez} residues Leu27, Glu42, Gln43 and Gly50, showing significant CSP in the fast exchange mode, were used in the global fit. ***D***, Individual titration curves for the same residues. K_D values are indicated in each plot. ***E***, Normalized CSP values of linear diubiquitin residues I3p (p = proximal ubiquitin), Leu8, Ile44, Lys63p, Val70 and Leu71, showing significant CSP in the fast exchange mode, were used in the global fit. ***F***, Individual titration curves for the Leu8, Ile44, Val70 and Leu71. K_D values are indicated in each plot. ***G***, Normalized CSP values of UBA^{Cez} residues Ser10, Leu27, Glu42, Gln43 and Gly50, showing significant CSP in the fast exchange mode, were used in the global fit. ***H***, Individual titration curves for the Ser10, Glu42, Gln43 and Gly50. K_D values are indicated in each plot.

Figure S7

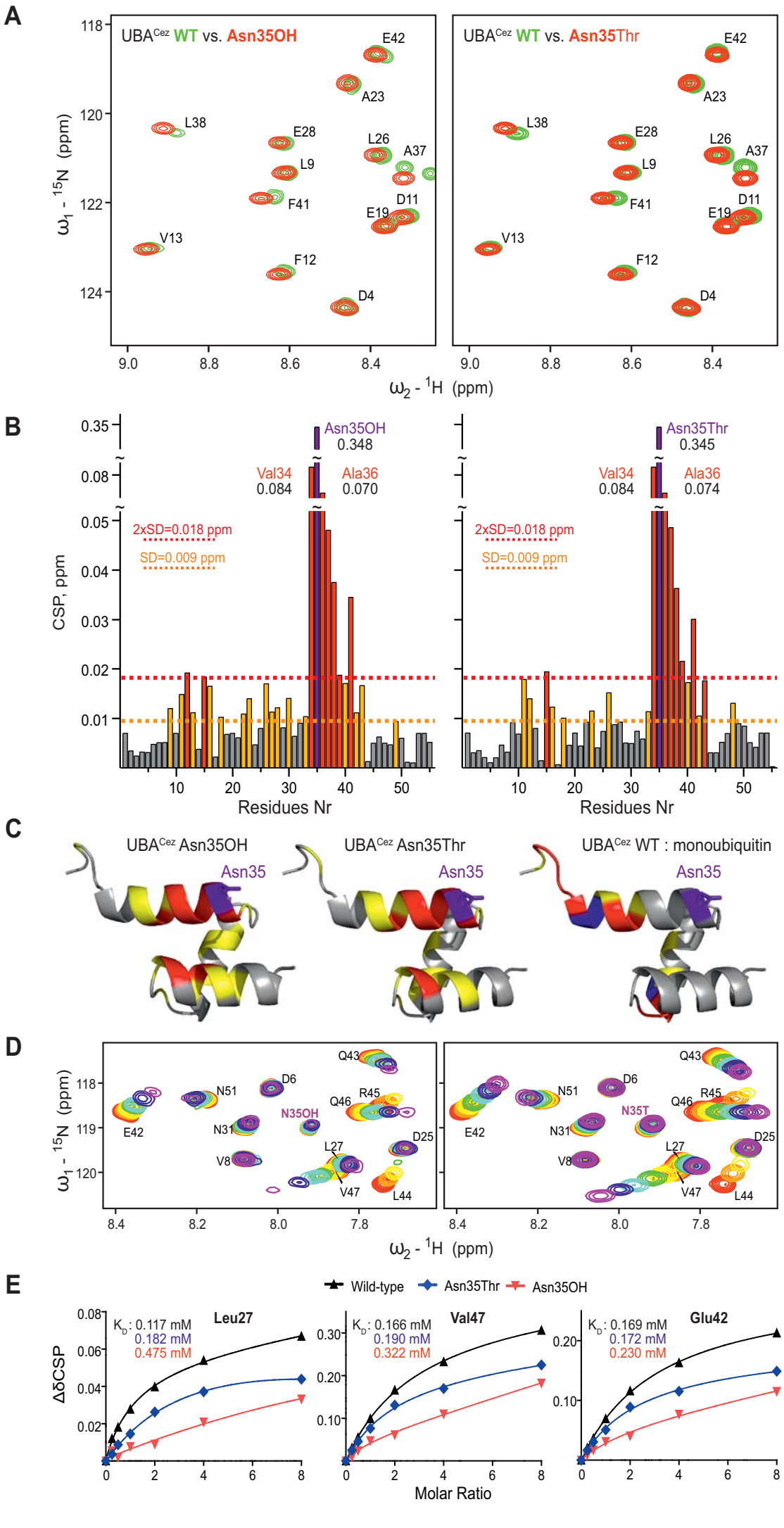
A
UBACez WT vs. Asn35OH
UBACez WT vs. Asn35Thr
E42
A23
L38
E28
L26
A37
L9
F41
D11
E19
V13
F12
D4
ω1 - 15N (ppm)
ω2 - 1H (ppm)
B
Asn35OH 0.348
Asn35Thr 0.345
Val34 0.084
Ala36 0.070
Ala36 0.074
2xSD=0.018 ppm
SD=0.009 ppm
CSP, ppm
Residues Nr
C
UBACez Asn35OH
UBACez Asn35Thr
UBACez WT : monoubiquitin
Asn35
D
Q43
N51
D6
R45
Q46
N35OH
N35T
N31
E42
V8
L27
D25
V47
L44
E
Wild-type
Asn35Thr
Asn35OH
Leu27
Val47
Glu42
KD: 0.117 mM
0.182 mM
0.475 mM
KD: 0.166 mM
0.190 mM
0.322 mM
KD: 0.169 mM
0.172 mM
0.230 mM
ΔδCSP
Molar Ratio

Figure S7: Binding of monoubiquitin to hydroxylated or mutated UBA^{Cez}. ***A***, NMR spectra of hydroxylated (Asn35OH) or mutated (Asn35Thr) UBA^{Cez} in comparison to wild-type UBA^{Cez}. Representative area of [^{15}N,^{1}H]-BEST-TROSY-HSQC spectra is shown for UBA^{Cez} wild-type (green) in overlay with UBA^{Cez} (Asn35OH) (left plot, red) and UBA^{Cez} (Asn35Thr) (right plot, red) spectra. Reproducible CSPs induced by hydroxylation or mutation are observed for residues sequentially distant from the modified Asn35, indicating changes in local structure and/or dynamics of the affected residues. ***B***, CSP mapping on the sequences of UBA^{Cez} variants. Yellow and red lines indicate 1× and 2× standard deviations (δ) calculated from CSP values of all residues, respectively. The CSP for hydroxylated/mutated Asn35 (purple) and its closest neighbors (Val34 and Ala36) are significantly bigger than for the other residues. Exact CSP values (in ppm) are given on the plots. ***C***, CSP induced by Asn35 hydroxylation (left) and Asn35Thr mutation (middle) are mapped on the modelled structure of UBA^{Cez}. Residues with intermediately ($\delta \leq CSP \leq 2\times\delta$) and strongly ($CSP \geq 2\times\delta$) perturbed backbone HN resonances are marked in yellow and red, respectively. Asn35 is highlighted in purple. The right plot shows the CSP induced by monoubiquitin titration to UBA^{Cez} (the same orientation). Importantly, the regions of UBA^{Cez} affected by Asn35 modification and by ubiquitin binding are overlapped. This fact indicates that Asn35 modification affects the residues directly interacting with ubiquitin. Indeed, NMR titration experiments for UBA^{Cez} with hydroxylated and mutated Asn35 showed their reduced affinity to ubiquitin. ***D***, NMR titration of ^{15}N-labelled UBA^{Cez} (Asn35OH) (left) and (Asn35Thr) (right) with monoubiquitin. Representative areas of [^{15}N,^{1}H]-BEST-TROSY-HSQC spectra are shown. The rainbow color code indicates increasing molar ratios upon titration from the free UBA^{Cez} (red) to UBA^{Cez} under 8 times molar excess of monoubiquitin (magenta). The CSP induced by monoubiquitin in both proteins are smaller in values and display faster exchange mode. ***E***, K_D values calculated for selected residues of hydroxylated (Asn35OH), mutated (Asn35Thr) and wild-type UBA^{Cez} upon titration with monoubiquitin. CSP values of residues Leu27, Glu42 and Val47 were used in the global fit. The K_D values for the wild-type UBA^{Cez} differ slightly from the values shown in Figure S6 due to another (less precise) titration scheme.